Spatially Specific Attention Mechanisms Are Sensitive to Competition during Visual Search

Lu-Chun Yeh, Yei-Yu Yeh, and Bo-Cheng Kuo

Abstract

■ Extensive studies have focused on selection mechanisms during visual search. One important influence on these mechanisms is the perceptual characteristics of the stimuli. We investigated the impact of perceptual similarity between targets and nontargets (T-N similarity) in a visual search task using EEG. Participants searched for a predefined target letter among five nontargets. The T-N similarity was manipulated with three levels: high, middle, and low. We tested for the influences of T-N similarity on an ERP (e.g., N2pc) and alpha oscillations. We observed a significant N2pc effect across all levels of similarity. The N2pc amplitude was reduced and occurred later for high similarity relative to low and middle similarities. We also showed that the N2pc amplitude was inversely correlated with the RTs across all similarities. Importantly, we found a significant alpha phase adjustment about the same time as the N2pc for high similarity; by contrast, no such effect was observed for middle and low similarities. Finally, we showed a positive correlation between the phase-locking value and the N2pc—the stronger the alpha phase-locking value, the larger the N2pc, when the T-N similarity was high. In conclusion, our results provide novel evidence for multiple competitive mechanisms during visual search. ■

INTRODUCTION

Goal-directed selection of visual items from the external environment relies upon our ability to identify stimulus properties that are most relevant to the task in hand, often while simultaneously ignoring behaviorally irrelevant distractions. Many studies have focused on selective mechanisms during visual search, isolating the cognitive and neural processes that enable us to identify the presence of a specific target among irrelevant nontargets or distractors (Eimer, 2014; Chelazzi, 1999; Wolfe, 1994; Duncan & Humphreys, 1989; Treisman & Gelade, 1980). The characteristics of visual stimuli can heavily influence the extent to which attention can be effectively allocated (Itti & Koch, 2001; Desimone & Duncan, 1995). The efficiency of searching for predefined targets may depend on the properties of surrounding objects. When distractors are more similar to one another, it is easier to identify the target. In addition, the perceptual similarity between targets and nontargets (T-N similarity) can also affect the efficiency of visual search—when targets are more dissimilar from the distractors, it is easier to find (Duncan & Humphreys, 1989). Here, we investigated how neural activity is modulated as we search for targets, using EEG, and in particular whether this is sensitive to T-N similarity.

There are many theoretical accounts of visual search (Eimer, 2014; Wolfe, 1994; Duncan & Humphreys, 1989; Treisman & Gormican, 1988), and most posit a strong role for the visual properties of the stimuli in the array or scene. According to one popular account (Kastner & Ungerleider, 2000, 2001; Desimone & Duncan, 1995), when multiple items are simultaneously presented in a visual display, they compete for neural representation through mutually suppressive interactions. According to this account, the processing capacity for visual information is limited, and this creates a bottleneck for selection. This competitive process can be biased via top–down mechanisms to ensure that relevant information is represented (Buschman & Kastner, 2015; Reynolds & Chelazzi, 2004; Kastner & Ungerleider, 2000; Desimone & Duncan, 1995; Bundesen, 1990). Evidence in favor of this account comes from many sources. Neurophysiological evidence in macaques has revealed that neuronal responses are reduced when two visual stimuli are simultaneously presented in the same receptive field of neurons in visual extrastriate areas (Reynolds & Chelazzi, 2004; Moran & Desimone, 1985). Studies in humans using fMRI also showed a reduction in the neural response in the visual cortex to stimuli under conditions of competition (Scalf & Beck, 2010; Beck & Kastner, 2009). These findings suggest that attention biases competitive interaction to the attended target in visual areas (Reynolds, Chelazzi, & Desimone, 1999; Luck, Chelazzi, Hillyard, & Desimone, 1997).

The time course of competitive bias toward target representations in visual search is relatively unclear. To address this, we exploited an ERP, namely, the N2pc, and

National Taiwan University

oscillatory activity in the alpha band (9–13 Hz) as indices of spatiotopically organized selection processes during visual search. The N2pc is typically observed between 200 and 400 msec after the onset of the search array, with more negative potentials over electrode sites contralateral to the attended hemifield (Eimer & Grubert, 2014; Töllner, Gramann, Müller, Kiss, & Eimer, 2008; Hopf et al., 2000; Luck & Hillyard, 1994). The N2pc is closely related to the selection of targets based upon template matching (Eimer & Grubert, 2014; Brignani, Lepsien, & Nobre, 2010; Kuo, Rao, Lepsien, & Nobre, 2009; Eimer, 1996). Other lateralized electrophysiological effects have also been linked with visual search. For example, oscillatory power in the alpha band at posterior brain regions shows decreased power contralateral to the attended hemifield and increased power contralateral to the unattended hemifield (Payne, Guillory, & Sekuler, 2013; Klimesch, 2012; Händel, Haarmeier, & Jensen, 2011; Rihs, Michel, & Thut, 2009; Sauseng et al., 2009; Kelly, Lalor, Reilly, & Foxe, 2006; Thut, Nietzel, Brandt, & Pascual-Leone, 2006; Worden, Foxe, Wang, & Simpson, 2000). One widely held view is that alpha power lateralization reflects a top–down modulation of neuronal excitability/inhibition that serves to gate incoming sensory information, with selective enhancement of targets and suppression of irrelevant nontargets or distractors (Payne & Sekuler, 2014; Zumer, Scheeringa, Schoffelen, Norris, & Jensen, 2014; Händel et al., 2011). Recent EEG studies using forward or inverted encoding models further suggest that alpha power topographies could covary with the exact location of an attended item rather than just the hemifield (Foster, Sutterer, Serences, Vogel, & Awh, 2017; Samaha, Sprague, & Postle, 2016). Similarly, the phase of alpha oscillation that reflects rhythmic changes of fluctuating states of neuronal excitability or inhibition has also been shown to modulate visual perception and awareness (Romei, Gross, & Thut, 2012; Dugué, Marque, & VanRullen, 2011; Busch, Dubois, & VanRullen, 2009; Mathewson, Gratton, Fabiani, Beck, & Ro, 2009). The adjustment of alpha phase may indicate the timing of the modulation by the top–down mechanisms in the visual cortex on a fast timescale (Jensen, Bonnefond, & VanRullen, 2012; Klimesch, 2012; Haegens, Nácher, Luna, Romo, & Jensen, 2011; Klimesch, Sauseng, & Hanslmayr, 2007).

Here, we investigated the electrophysiological correlates of T-N competitive interactions during visual search. T-N similarity was manipulated with three levels: high, middle, and low. The more similar the nontargets are to the target, the more they should compete with it for representation. As a result, the degree of top–down bias needed in order to select the target should increase. If either the N2pc or alpha oscillation reflects this process, then it should be influenced by T-N similarity. Moreover, we conducted a model-based analysis (van den Berg, Appelbaum, Clark, Lorist, & Woldorff, 2016; Myers, Stokes, Walther, & Nobre, 2014) to explore the relationships between N2pc and search performance on a trial-by-trial basis. We also tested for the relationship between the N2pc and alpha oscillation for visual search. Differential relationships between the neural markers and between brain activity and behavior could provide strong evidence for the roles of these two mechanisms (e.g., N2pc and alpha oscillations) in visual search.

METHODS

Participants

Twenty healthy volunteers (12 women, age range = 20–27 years, mean age = 22.25) participated in this study. All participants were right-handed according to the Edinburgh Handedness Inventory (Oldfield, 1971). The participants had normal or corrected-to-normal visual acuity, provided informed written consent before the experiment, and were financially reimbursed for their time (500 NTD, about 16 USD). All experimental methods and procedures were approved by the research ethics Office of the National Taiwan University.

Stimuli

Stimuli were presented on a 17-in. cathode ray tube monitor with a refresh rate of 60 Hz using the E-Prime software (Psychology Software Tools, Inc.). We selected 12 English letters based on the similarity measures of letter identification from previous findings (Mueller & Weidemann, 2012; Townsend, 1971). The target letters were X and N (Lavie & Cox, 1997). The similar nontarget letters with linear characteristics included H, K, M, V, and Y; the dissimilar nontarget letters with curved characteristics included C, G, O, Q, and D. Each letter stimulus subtended a visual angle of approximately 0.42° (height) × 0.42° (width) and was presented in white, capital Courier New font. The target and nontarget letters were positioned in six possible peripheral locations of an invisible circle that subtended approximately 1.87° in radius with equal space between adjacent letters. All of the stimuli were presented against a black background.

Task Design

The experimental design followed a 3 (T-N similarity: high, middle, low) × 2 (target side: left, right) within-subjects factorial design. The five nontarget letters with linear characteristics were presented for high-similarity trials, and the five nontarget letters with curve-shaped characteristics were presented for low-similarity trials. Three curve-shaped nontarget letters and two linear nontarget letters were presented for middle-similarity trials. The relative locations among the target letter and linear and curve-shaped nontarget letters were fully counterbalanced. The task procedure is illustrated in Figure 1.

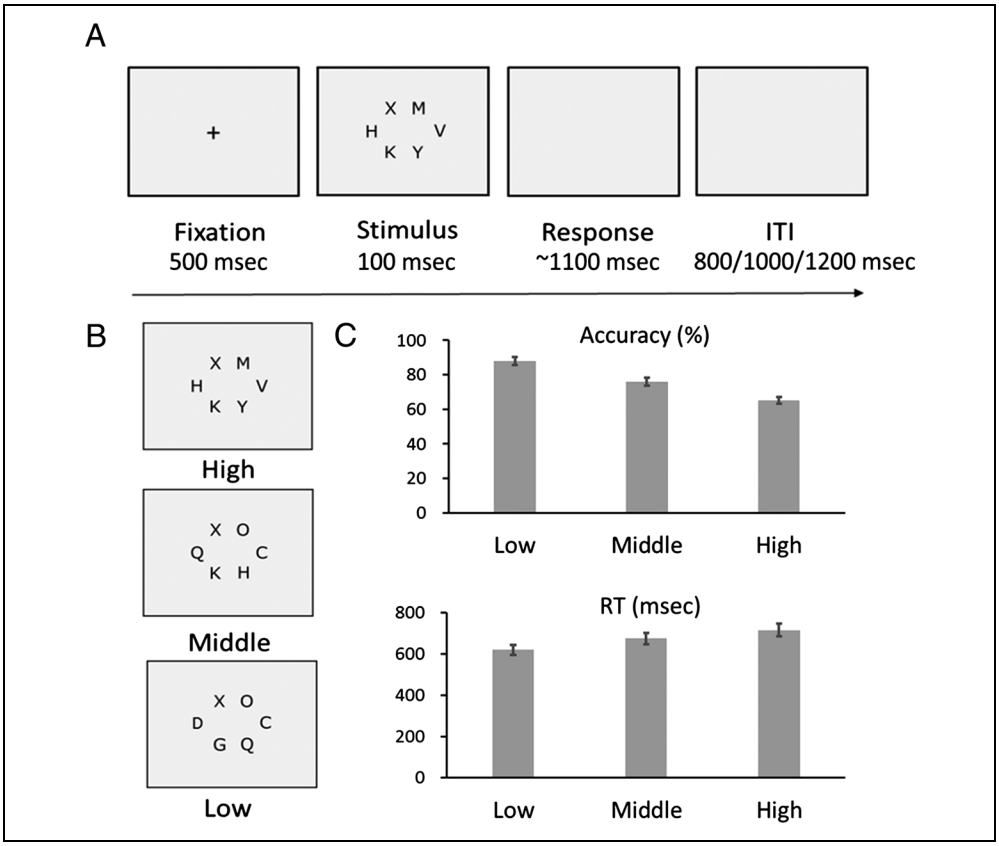

Figure 1. (A) Schematic illustration of the visual search task. Participants were instructed to search for a predefined target letter (X or N) from within a search array and to ignore the nontarget letters (ITI = intertrial interval). (B) The T-N similarity was manipulated with three levels (high, middle, and low). The five nontarget letters with linear characteristics were presented for high-similarity trials, and the five nontarget letters with curve-shaped characteristics were presented for low-similarity trials. Three curve-shaped nontarget letters and two linear nontarget letters were presented for middle-similarity trials. (C) Behavioral results including mean accuracy (%) and RT (msec). Error bars represent the standard errors of the means.

Each trial began with the onset of a centrally displayed fixation for 500 msec, which signaled the onset of the trial. After that, a search array consisting of six stimulus letters was presented for 100 msec and followed by a maximal 1100 msec for response. Participants were instructed to search for a predefined target letter (X or N) and ignore the nontarget letters. Half of the participants were instructed to press the left mouse button for the target "X" using their left thumb and the right mouse button for the target "N" using their right thumb, whereas the other half were instructed oppositely. The interval between trials varied randomly between 800, 1000, and 1200 msec.

Experimental Procedure

Participants were comfortably seated in a dimly illuminated room, facing a cathode ray tube monitor placed 57 cm in front of them. Before the formal experiment, the participants were given written, as well as verbal, instructions about the task requirements. Participants first completed a practice block of 36 trials to ensure that they could perform the task as instructed. They were encouraged to rest between blocks that they could self-initiate. In the formal experiment, all trial types were equiprobable and randomized within 30 blocks of 36 trials, yielding 1080 trials in total (360 trials for each high-, middle-, and low-similarity condition). Participants were instructed to maintain fixation on a small fixation marker at the center of the screen during the experimental trials and to respond as quickly and accurately as possible. Participants responded using both hands by pressing the mouse buttons. The participants were also asked to minimize blinking and movement of their eyes while performing each trial throughout the experiment. The total experimental time for each participant was approximately 60 min.

Behavioral Analyses

The behavioral measures, including accuracy and RTs, were each analyzed by one-way (T-N similarity: high, middle, low) repeated-measures ANOVA. Only correct responses were included in the RT analyses.

EEG Acquisition

The EEG data were recorded continuously using a NuAmp amplifier (Neuroscan, Inc.), with 37 Ag/AgCl electrodes placed on the scalp with an elasticated cap positioned according to the 10–20 international system. The montage included six midline sites (Fz, FCz, Cz, CPz, Pz, and Oz) and 12 sites over each hemisphere (FP1/FP2, F3/F4, F7/F8, FC3/FC4, FT7/FT8, C3/C4, T3/T4, CP3/CP4, TP7/TP8, P3/P4, T5/T6, and O1/O2). Vertical eye movements were recorded by electrodes placed on the

supraorbital and infraorbital ridges of the right eye (vertical EOG [VEOG]), and horizontal eye movements were recorded by electrodes placed on the outer canthi of the right and left eyes (horizontal EOG [HEOG]). Additional electrodes served as the ground (AFz, positioned between FPz and Fz) and reference (A1 and A2 mastoid sites, with A2 serving as the active online reference). Electrode impedances were kept below 5 KΩ. Ongoing brain activity at each electrode site was sampled every 1 msec (1000-Hz analogue-to-digital sampling rate). The activity was filtered with a low-pass filter of 300 Hz, and no high-pass filter was used. Digital stimulus presentation codes were sent to the EEG acquisition computer via a parallel port from the stimulus presentation computer, indicating the type and exact time of presentation for each event.

EEG Preprocessing

Offline, the EEG data were re-referenced to the algebraic average of the right and left mastoids (A1 and A2). Bipolar EOG signals were derived by computing the difference between the voltages at electrodes placed to the side of each eye (HEOG) and above and below the left eye (VEOG). The continuous EEG data were then segmented into epochs starting 500 msec before and ending 1000 msec after the onset of the stimuli. The EEG epochs were baseline-corrected, with a 100-msec prestimulus period. Epochs containing excessive noise or drift (±100 μV) at any electrode were excluded. Epochs with ocular artifacts (blinks or saccades) were also rejected in two steps. Blinks were identified as large deflections (±60 μV) in the HEOG or VEOG electrodes. Visual inspection was then carried out to confirm the appropriate removal of artifacts and identify residual saccades or eye movements (e.g., boxcar-shaped voltage deflection) in individual HEOG traces (±10–20 μV). Trials with incorrect behavioral responses were also discarded from further analyses.

Epochs were then averaged according to T-N similarity and target side. For each condition, ERPs were derived from the onset of the search arrays. ERPs from trials containing targets located on the right and from trials containing targets located on the left side were combined by an averaging procedure that preserved the electrode location relative to the target side (contralateral or ipsilateral side to the target). To maintain an acceptable signal-to-noise ratio, a lower limit of 100 artifact-free trials per subject per condition was set.

ERP Analysis

We first tested for the occurrence of the N2pc potential across three types of T-N similarity. Statistical analyses for the N2pc were performed using the mean voltage value (mean amplitude) over successive time bins across different scalp regions. The mean amplitudes of the N2pc were measured between 200 and 320 msec at the occipital-temporal electrodes (e.g., the averaged amplitude of T5/T6 and TP7/TP8) contralateral and ipsilateral to the side of the target (e.g., Eimer, 1996; Luck & Hillyard, 1994). To test the time course of the influences of T-N similarity on visual search, we divided 200–320 msec into three time windows: 200–240 msec, 240–280 msec, and 280–320 msec. A three-way repeated-measures ANOVA was computed of the mean amplitudes of the N2pc, testing the effects of T-N similarity (high, middle, low), Time window (200–240 msec, 240–280 msec, 280–320 msec), and Target side (contralateral and ipsilateral to target). Only effects including the factor of Target side, reflecting differential activity observed in ipsilateral versus contralateral electrodes, were of interest. We also confirmed the N2pc effect (ipsilateral side relative to contralateral side to target) for each similarity condition for each time window using paired t tests. The Greenhouse–Geisser epsilon correction for nonsphericity was applied to all ERP analyses where appropriate (Jennings & Wood, 1976), and only corrected probability values and degrees of freedom are reported.

Relationship between N2pc and RTs

We conducted a model-based analysis (Myers et al., 2014) to test for the relationship between the N2pc and the RTs at two levels. At the individual level, we calculated the N2pc by subtracting the amplitude at the contralateral side from the ipsilateral side relative to the target location for each trial for each of three time windows (200–240 msec, 240–280 msec, 280–320 msec), respectively. We fitted a general linear model (GLM) to the z-transformed N2pc amplitude using the z-transformed RT as a regressor at each of time point for each electrode of interest (e.g., T5/T6 and TP7/TP8) for each N2pc time window on a trial-by-trial basis. The GLM was fitted for each of the T-N similarity conditions separately and then averaged regression weights (beta estimates) across conditions and the electrodes of interest. This was repeated for each participant's ERP data. Individual data were then entered into the group-level analysis. We used one-sample t tests to examine a significant relationship between N2pc and RTs ($p < .05$, two-tailed). In essence, this tests whether the variability in RT is significantly predicted by the trial-wise variability in the magnitude of the N2pc effect.

EEG Time–Frequency Analysis

Offline EEG time–frequency analyses were performed using SPM12 software (Wellcome Trust Centre for Neuroimaging, University College London, UK) and Fieldtrip toolbox (Oostenveld, Fries, Maris, & Schoffelen, 2011) in MATLAB (MathWorks) complemented by in-house MATLAB scripts. The epoched EEG signals were downsampled to 250 Hz and entered into a time–frequency

decomposition using continuous Morlet wavelet transformation with a length of seven cycles. Time–frequency representations of power and phase were estimated for each trial, electrode, and participant across a frequency range between 1 and 20 Hz in 1-Hz steps. The resulting time–frequency power spectrograms were averaged across the trials according to the T-N similarity for each participant. The power estimates were then log-transformed and rescaled to the baseline relative to −200 to −100 msec preceding the search onset using LogR method in SPM12 (log10(p/p_b)) (p: power of the trial; p_b: power in the baseline). Moreover, phase-locking values (PLVs) were also calculated for each participant using the following equation (Bonnefond & Jensen, 2012; Tallon-Baudry, Bertrand, Delpuech, & Pernier, 1996):

$$\mathrm{PLV} = \frac{1}{N}\left|\sum_{k=1}^{N} e^{i\varphi^{k}(f,t)}\right|$$

where N is the number of trials and $\varphi^{k}(f, t)$ provides complex polar representation at frequency f and time point t on trial k. The PLV varies from 0 to 1, where 0 indicates strong variability of phase angles across trials whereas 1 indicates that all trials have the same phase angle at given frequency and time point. Thus, the PLV reflects the extent to which phase angles are consistent over trials at that point in the time–frequency space.

The statistical analyses were computed using a cluster-based nonparametric permutation approach (Maris & Oostenveld, 2007) across participants for each T-N similarity condition. This analytical approach controlled for Type I errors by calculating the size of any significant clusters with consecutive t tests that were significant ($p < .05$) across neighboring electrodes, time points, or both, with averaging across the alpha band (9–13 Hz). For the statistical analysis of lateralized power and PLVs in the alpha range for each T-N similarity condition, we compared the differences between the ipsilateral versus contralateral to the target hemifield after the offset of the search array. We then tested the statistical significance using dependent sample t tests by calculating Monte Carlo p values on 1000 random partitions, in which two conditions were shuffled to create the null distribution of the clustered test statistics that would be achieved by chance. We estimated the corrected p value according to the proportion of the null distribution exceeding the observed cluster-level t statistics. If its size was unlikely to have occurred by chance ($p < .05$, two-tailed), the cluster was treated as significant.

Correlation between Lateralized Alpha Power/PLVs and N2pc

We also tested for the relationship between the lateralized alpha power/PLVs and the N2pc in the model-based analysis at the group level. For each time window of N2pc and for each of the T-N similarity conditions, we fitted the GLM to the z-transformed lateralized alpha power and PLVs (averaged 9–13 Hz and electrodes of interest), respectively, using the z-transformed mean N2pc (averaged electrodes of interest) as a regressor. Three N2pc effects (from 200 to 240 msec, from 240 to 280 msec, and from 280 to 320 msec) were used to fit each GLM. We then evaluated the strength of correlation between lateralized alpha power and N2pc and between lateralized alpha PLV and N2pc on the basis of a jackknife approach (Miller, Patterson, & Ulrich, 1998). We iteratively removed one participant from all the participants and thus resulted in 20 data sets. This leave-one-participant-out approach allows us to obtain a jackknife estimate of the reliability of the correlation and the estimate of the standard error allows us to compare the beta estimates against zero (i.e., the null hypothesis of no correlation) using one-sample t tests and the Type I error were corrected using Bonferroni correction for three time windows ($p < .0167$, two-tailed).

Analysis of Temporal Relationship between Lateralized Alpha PLV and N2pc

Finally, we explored the temporal relationship between the time courses of lateralized alpha PLV and N2pc for high similarity using a cross-correlation analysis (van Ede, Chekroud, Stokes, & Nobre, 2019). We calculated the cross-correlational coefficients between these two time courses from 200 to 320 msec using the *xcov* function in MATLAB for each participant. We set the range of time lag from −40 to 40 msec, shifting PLV time course in a 4-msec step on the basis of the N2pc time course. The cross-correlation coefficient varies from −1 to 1, where 1 (−1) indicates positive (negative) correlation between two signals and 0 indicates no correlation. The maximal coefficient at negative or positive time lag indicates the temporal difference in correlation between the time courses of lateralized alpha PLV and N2pc (negative time lag: lateralized alpha PLV occurs before the N2pc; positive time lag: the N2pc occurs before the lateralized alpha PLV). On the other hand, the maximal coefficient at zero lag indicates no temporal difference between the two time courses. The cross-correlation coefficients were transformed to z values using Fisher's z transform for each participant. We used one-sample t tests ($p < .05$, one-tailed) to compare the Fisher's z scores against zero (i.e., the null hypothesis of no correlation) for each time lag. If the lateralized alpha PLV occurs preceding the N2pc for high similarity, we would expect maximal correlation between the two time courses at negative time lag.

RESULTS

Behavioral Results

The behavioral results are illustrated in Figure 1. The accuracy data showed a significant main effect of T-N similarity, $F(2, 38) = 181.496$, $p < .001$, $\eta_p^2 = .905$. Tukey's

honestly significant difference post hoc comparisons indicated that the low-similarity condition (M = 0.88, SE = 0.023) was more accurate than the middle- (M = 0.76, SE = 0.023) and high-similarity (M = 0.65, SE = 0.02) conditions, and the middle-similarity condition was more accurate than the high-similarity condition. The analysis of RT data revealed a significant main effect of the T-N similarity, $F(2, 38) = 63.146$, $p < .001$, $\eta_p^2 = .769$. Post hoc comparisons indicated that the RTs for the low-similarity condition (M = 620.25, SE = 25.206) were faster than those for the middle- (M = 675.69, SE = 27.652) and high-similarity (M = 715.85, SE = 31.51) conditions, and those of the middle-similarity condition were also faster than those of the high-similarity condition. These results demonstrated the influence of T-N similarity on visual search performance—as targets and distractors became more similar, subjects became slower and more error prone in their search.

ERP Results

The ERP results are shown in Figure 2. The ERP results showed a significant main effect of Target side, $F(1, 19) = 41.90$, $p < .001$, suggesting an N2pc effect. We also observed significant main effects of Time window, $F(1.377, 38) = 5.46$, $p = .019$, significant two-way interactions between the T-N similarity and Time window, $F(3.059, 76) = 12.52$, $p < .001$, Target side and Time window, $F(1.632, 38) = 27.36$, $p < .001$, T-N similarity and Target side, $F(2, 38) = 13.31$, $p < .001$, and a significant three-way interaction among T-N similarity, Target side, and Time window, $F(2.729, 76) = 9.79$, $p < .001$. To clarify these interactions and the N2pc effects, we tested the impact of T-N similarity on the N2pc for each time window in the follow-up analyses below.

For the time window of 200–240 msec, the N2pc effects were significant for the middle-, $t(19) = 2.47$, $p = .023$, and low-similarity, $t(19) = 3.67$, $p = .002$, trials. The difference in N2pc amplitudes among the three types of similarity, however, was not significant during this time window, $F(2, 38) = 1.86$, $p = .17$. Next, we observed significant N2pc effects for the high-, $t(19) = 2.30$, $p = .033$, middle-, $t(19) = 4.72$, $p < .001$, and low-similarity, $t(19) = 5.16$, $p < .001$, trials during 240–280 msec and significant N2pc effects for the high-, $t(19) = 2.66$, $p = .015$, middle-, $t(19) = 4.86$, $p < .001$, and low-similarity, $t(19) = 6.69$, $p < .001$, trials during 280–320 msec. Finally, we found a significant effect of the T-N similarity

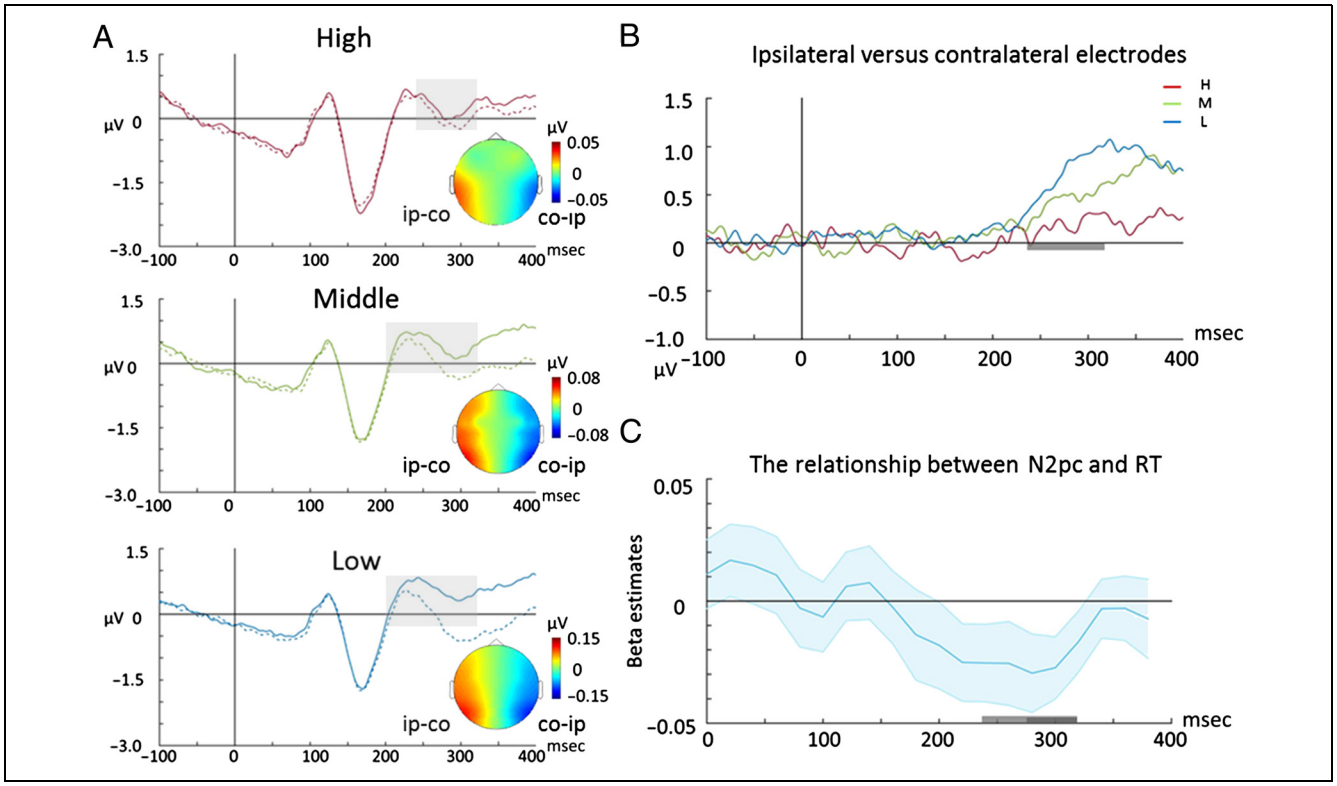

Figure 2. (A) ERP waveforms averaged across all participants are shown for the three conditions over posterior brain regions. The N2pc was elicited between 200 and 320 msec at the occipital-temporal electrode pairs (T5/6 and TP7/8) contralateral (co, waveforms: dashed lines; topographies: blue/right side) and ipsilateral (ip, waveforms: solid lines; topographies: red/left side) to the side of the target. Shadow in gray represents the significant time windows. (B) The voltage difference between the ipsilateral and contralateral side is also shown for high similarity (H: red line), middle similarity (M: green line), and low similarity (L: blue line), respectively. The ERP waveforms were low-pass filtered (40 Hz) for illustration purposes. (C) A significant correlation between the N2pc and the RT across three conditions was found at the time windows of 240–280 msec (light gray) and 280–320 msec (dark gray). Shadow represents the standard errors of the means.

on the N2pc amplitude from 240 to 280 msec, $F(2, 38) = 11.56$, $p < .001$, and from 280 to 320 msec, $F(2, 38) = 17.86$, $p < .001$. These results showed a reduction in the N2pc amplitude during the high-similarity trials relative to that of the low-similarity trials from 240 to 320 msec and a reduction in the N2pc amplitude during the high-similarity trials relative to the middle-similarity trials from 280 to 320 msec. No significant differences in the N2pc effect between the low- and middle-similarity trials were found across the three time windows.

Relationship between N2pc and RTs

Next, we conducted a trial-by-trial model-based analysis to test for the relationship between the N2pc and the RTs. We showed a significant negative relationship between the N2pc and RTs during the time window of 240–280 msec ($p = .004$) and 280–320 msec ($p < .001$). These results showed that N2pc amplitude was inversely correlated with the RTs across all similarity conditions—the bigger the N2pc, the faster the RT on that trial (Figure 2C).

EEG Time–Frequency Results

We then tested whether the T-N similarity can influence lateralized power and PLVs in the alpha band (ipsilateral vs. contralateral side). We identified a significant effect for high T-N similarity trials with increased PLV over the ipsilateral side to the target location and decreased PLV over the contralateral side to the target location, which began at 224 msec and extended to 276 msec (corrected $p = .027$), over occipital-temporal electrodes (T5/6 and TP7/8). However, no such effect was observed for the middle- and low-similarity trials. We did not observe any significant effect for lateralized alpha power for all three types of similarity. The time–frequency results are illustrated in Figure 3.

Correlation between Lateralized Alpha Power/PLVs and N2pc

We tested for the relationship between lateralized alpha power/PLVs and N2pc for the high T-N similarity trials. We found that the strength of lateralized PLV (ipsilateral vs. contralateral side) was positively correlated with the N2pc amplitude (ipsilateral vs. contralateral side) from 240 to 280 msec, $t_c(19) = 4.97$, $p < .001$, and from 280 to 320 msec, $t_c(19) = 4.93$, $p < .001$ (Figure 4A). No other significant effect was observed.

Temporal Relationship between Lateralized Alpha PLV and N2pc

Finally, we calculated cross-correlations between the time courses of lateralized alpha PLV and N2pc for each

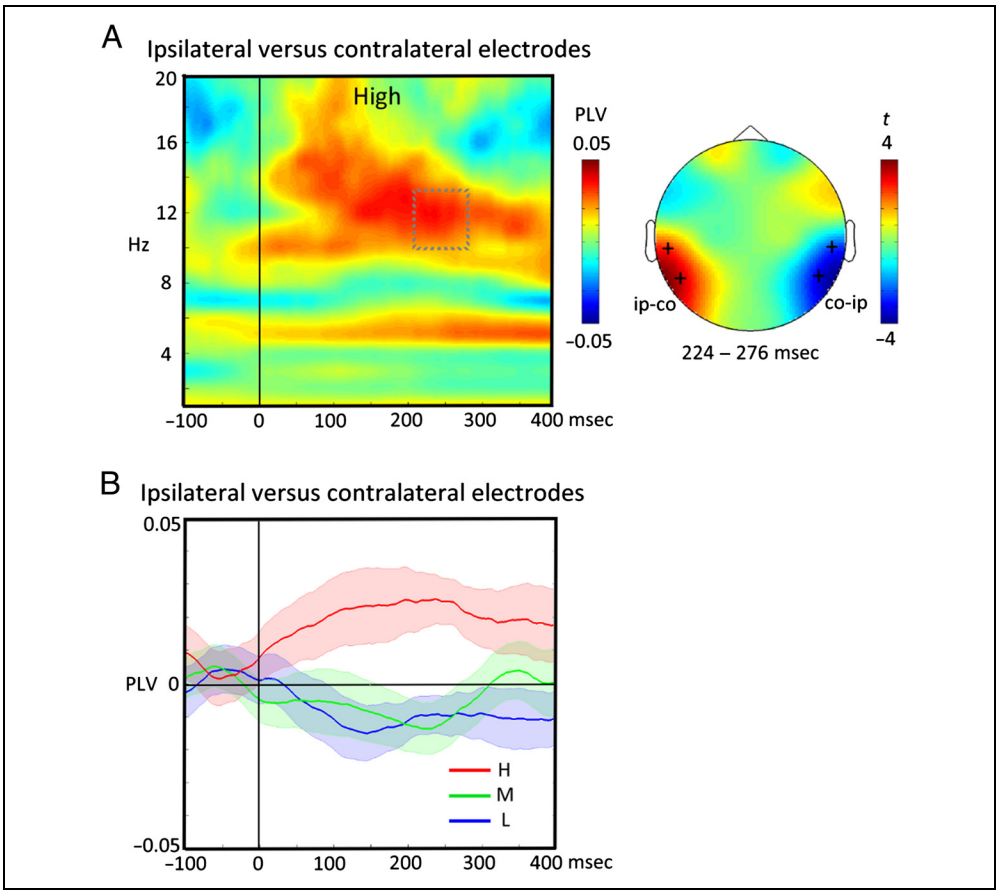

Figure 3. (A) The phase lateralization (ipsilateral vs. contralateral to the target location) over occipital-temporal electrodes (T5/6 and TP7/8, left) was observed during visual search for high T-N similarity. The temporal window for the significant effect is indicated by a square. The topographic map shows the symmetrical relative difference in PLV (right), with increased PLV over the ipsilateral (ip) scalp and decreased PLV over the contralateral (co) scalp. Blue indicates negative PLVs, and red indicates positive PLVs. (B) The differences in PLV between the ipsilateral and contralateral electrodes are illustrated for high similarity (H: red line), middle similarity (M: green line), and low similarity (L: blue line).

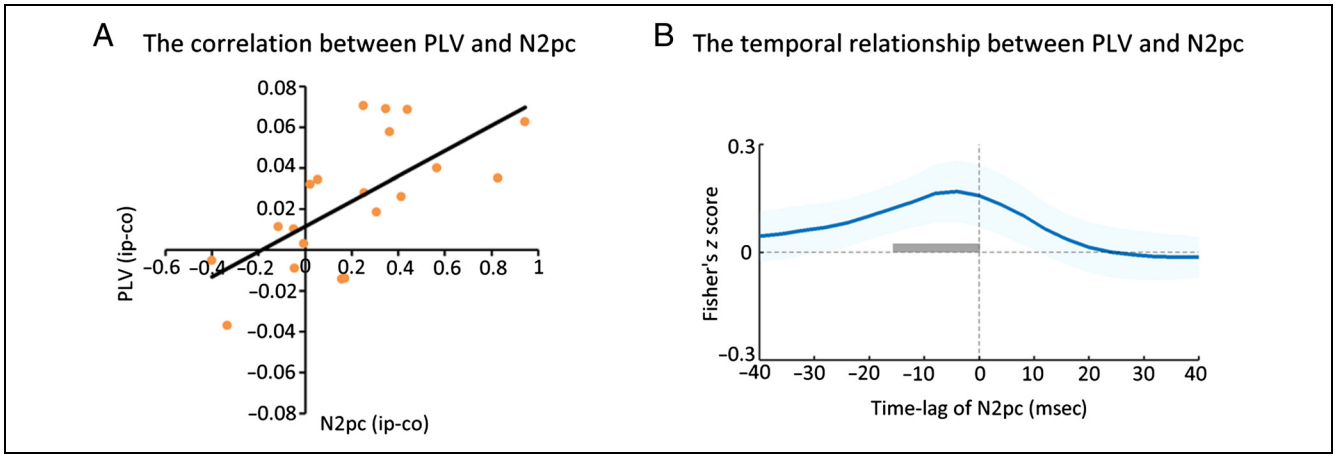

Figure 4. (A) We evaluated the strength of correlation between lateralized alpha power and N2pc and between lateralized alpha PLV and N2pc on the basis of a jackknife approach. A significant correlation between the N2pc (averaged from 240 to 320 msec) and the PLV (averaged from 224 to 276 msec) was found for high similarity. We showed the scatterplot and regression line for the relationship between PLV and N2pc for illustration purposes. (B) Cross-correlation coefficients between the time courses of lateralized alpha PLV and N2pc were evaluated for each participant. We set the range of time lag from −40 to 40 msec, shifting PLV time course in a 4-msec step on the basis of the N2pc time course. The maximal coefficient at negative or positive time lag indicates the temporal difference in correlation between the time courses of lateralized alpha PLV and N2pc. We found that the strength of lateralized PLV was positively correlated the N2pc amplitude from −16 to 0 msec time lags of N2pc ($ps < .05$; gray bar), but no significant effect was found at other time lags. Shadow represents the standard errors of the means.

participant. We found that the strength of lateralized PLV was positively correlated with the N2pc amplitude from −16 to 0 msec time lags of N2pc ($ps < .05$), but no significant effect was found at other time lags. The cross-correlational results are illustrated in Figure 4B.

DISCUSSION

The current study aimed to investigate the influences of T-N similarity on the electrophysiological activity during visual search. Three levels of T-N similarity, namely, high, middle, and low, were manipulated. Our ERP results showed a significant N2pc effect across all levels of T-N similarity. Particularly, the N2pc amplitude was reduced and occurred later for high similarity relative to those for low and middle similarities. We also showed a close relationship between N2pc and behavior. This result indicated that the N2pc amplitude was inversely correlated with the RT across all similarity conditions. Importantly, we found a significant lateralization of alpha phase-locked effect about the same time as the N2pc for high T-N similarity, but no such lateralization was observed for middle or low T-N similarities. Finally, we showed a positive correlation between the lateralized PLV and the N2pc—the stronger the PLV in the alpha band, the larger the N2pc, when the T-N similarity was high.

As a large body of ERP evidence has shown that the contralateral N2pc is elicited by the presence of task-relevant attributes during visual search (Eimer, 1996, 2014; Luck & Hillyard, 1994), we found N2pc effects across all levels of T-N similarity. The N2pc reflects a selective process that indicates the spatiotopic layout of a putative target map that results from preferential processing of the relevant representations of the target identity, that is, attentional templates (Grubert & Eimer, 2015; Nako, Smith, & Eimer, 2015). The presence of the N2pc across the three types of T-N similarity suggested the top–down selection of spatiotopic sensory codes based on template matching occurs in all conditions. But this process is variable across trials, and this variability mirrors target detection times—when the N2pc is large, it corresponds to targets being found more quickly. ERP studies that have combined visual search with cueing paradigms have shown that the N2pc is related to the selection of the visual target at specific locations instead of anticipatory attention per se (Woodman, Arita, & Luck, 2009; Kiss, Van Velzen, & Eimer, 2008). When observers search for a predefined target among multiple elements from within a stimulus array, a target template can guide allocation of attention for target selection (Olivers, Peters, Houtkamp, & Roelfsema, 2011; Duncan & Humphreys, 1989).

In accordance with the predictions based on the competition account (Desimone & Duncan, 1995), we showed that search efficiency was influenced by the T-N similarity. The behavioral performance suggested that searching was less efficient when the targets and nontargets were highly similar. The pattern of the ERP (i.e., the N2pc) mirrored the pattern of search performance, suggesting a later and reduced N2pc, as well as slower and less accurate searching, for high-similarity trial relative to that for middle- and low-similarity trials. ERP studies that have manipulated distractor heterogeneity demonstrated reduced N2pc amplitudes when targets were presented in more heterogeneous, random context relative to less heterogeneous, grouped context

(Feldmann-Wüstefeld & Schubö, 2015; Feldmann-Wüstefeld, Wykowska, & Schubö, 2013). In line with these findings, the reduction in the N2pc for high-similarity trials in the current study may reflect the competitions of neural representations during the target selection process (Hilimire, Mounts, Parks, & Corballis, 2009)—this competition takes longer to resolve, reflecting a slowed template matching conclusion alongside increased RTs. Similar nontarget stimuli may activate part of the target representations and this in turn causes the competition (cf. Bundesen, 1990). Such competition results in mutual suppression to degrade the preferential processing of target selection and makes the search process less efficient.

Importantly, a novel finding shows that alpha phase adjustment is also sensitive to the competition during visual search. The cortical rhythm in the alpha band can adjust in phase over posterior brain sites only when T-N similarity was high, with increased PLV in the ipsilateral site and decreased PLV in the contralateral site relative to the target location. This modulation of T-N similarity of PLV began approximately 224 msec after the onset of the search array. This effect was not present for the middle- or low-T-N-similarity trials. This finding is consistent with the notion that the alpha oscillation consists of a selective mechanism for enhancing relevant attributes and a suppressive mechanism for keeping irrelevant nontargets or distractors from limited neural representations (Kuo, Li, Lin, Hu, & Yeh, 2017; Payne et al., 2013; Jensen et al., 2012; Klimesch, 2012; Haegens et al., 2011; Rihs et al., 2009; Sauseng et al., 2009; Klimesch et al., 2007; Kelly et al., 2006; Thut et al., 2006; Worden et al., 2000). An adjustment in alpha phase may provide a modulatory mechanism for inhibiting nontarget items or distractors on a fast timescale for target selection. The positive correlation in the lateralized measurement (ipsilateral vs. contralateral side to the target location) between the PLV and N2pc for the high-similarity trial validated this view, suggesting a greater difference in alpha phase adjustment with a larger difference in the N2pc. One possibility is that this early effect in alpha phase reflects the early biasing of sensory processing. Under conditions of maximal competition a stronger bias is needed.

Although the PLV (from 224 msec) seems to occur earlier than the N2pc (from 240 msec) when the targets and nontargets were highly similar, the temporal relationship between these two signals is unclear. To address this issue, we calculated cross-correlational coefficients between the time courses of the lateralized alpha PLV and N2pc and observed the maximal positive correlations at negative time lags from −16 to 0 msec of N2pc. This analysis of time courses reflects that the lateralized alpha PLV could occur preceding or at the same time as the presence of N2pc but not later than the N2pc for high-similarity trials. These results also suggest that searching for a target among competitive nontargets triggers two distinct mechanisms of top–down control: alpha oscillation and N2pc. A recent study using a visual search paradigm provided complementary evidence to highlight this point of view (Bacigalupo & Luck, 2019). In their study, both N2pc and lateralized alpha suppression in power were observed when the target was presented in the lower visual field. These two lateralized effects also exhibited different time courses and responded differently to the effects of visual crowding. In line with their findings, we found that the alpha phase adjustment can also be partly dissociated from the N2pc in time and both N2pc and lateralized alpha PLV responded differently to T-N similarity.

Our results suggest that both top–down and bottom–up characteristics drive the priority in selection during visual search. Goal-relevant target templates hold in working memory bias selection toward the locations of stimuli that share similar features with the templates. Bottom–up characteristics such as stimulus saliency and the heterogeneity of search context also contribute to the computation in the priority map. The priority value influences the signal-to-noise ratio for selecting a target (see Zelinsky & Bisley, 2015, for detailed discussion of priority maps). On the low similarity trials, the priority assigned to the target was high because nontargets were dissimilar to the templates and were homogeneous. By contrast, the priority of the target was low on the high-similarity trials because nontargets were highly similar to the templates and were heterogeneous. The low signal-to-noise ratio on the high-similarity trials led to reduced N2pc while suppressing similar nontargets with high priority via lateralized alpha PLV approximately the time of selection. With stronger suppression, the N2pc became larger on the high-similarity trials.

Although we have been highlighting the distinct functions of alpha oscillation and N2pc during visual search as T-N similarity was varied, the distractor positive (Pd) that presents a positive going deflection contralateral to the distracting items is frequently reported in the literature of visual search (Hickey, Di Lollo, & McDonald, 2009). Several studies suggest that the Pd reflects a process to active suppression of a salient distractor (Feldmann-Wüstefeld & Vogel, 2019; Gaspelin & Luck, 2018a, 2018b; Sawaki, Geng, & Luck, 2012). We did not expect the occurrence of the Pd because no salient distractor was presented in search array. It is worth noting that the temporal relationship between the N2pc and Pd varied across different experiments. For example, ERP studies have revealed that the Pd may occur before (Feldmann-Wüstefeld & Vogel, 2019; Gaspelin & Luck, 2018a), after (Sawaki et al., 2012), or about the same time (Feldmann-Wüstefeld, Uengoer, & Schubö, 2015; Munneke, Fait, & Mazza, 2013) as the presence of the N2pc. Together with current results, these findings support the dynamic nature of top–down control mechanisms by which active suppression may interlink to the processes of target selection timely depending upon the task contexts or demands.

Taken together, our findings suggest the presence of dynamic and multiple competitive mechanisms during visual search. One mechanism of the search process is to allocate attention toward all possible target candidates and gate information by inhibition (Payne et al., 2013; Jensen & Mazaheri, 2010). When a search array appears, the neural populations in the visual cortex are tuned to the location of potentially relevant items, according to the current task goals (in our case, X and N). This process is influenced by the perceptual similarity of surrounding items within the search array. For example, when the T-N similarity is high, the target suffers strong competition from highly similar nontargets. This process thus allows for active inhibition or disengagement from irrelevant nontargets or distractors—the stronger the competition, the more strongly this information will need to be gated. We propose that this process corresponds to the spatially specific modulation of the alpha rhythm (Kuo et al., 2017; Payne et al., 2013; Klimesch, 2012; Händel et al., 2011; Rihs et al., 2009; Kelly et al., 2006; Thut et al., 2006; Worden et al., 2000). When targets and distractors compete more directly with one another, this spatiotopic modulation of sensory representations will need to be stronger. Another mechanism of search is to access the identity of target representations (Drisdelle & Jolicoeur, 2018; Aubin & Jolicoeur, 2016; Mazza, Turatto, & Caramazza, 2009). This mechanism allows for the reactivation of the neural ensembles coding for the target templates in working memory and the selection of the item that is best matched to the target template. The identification of target items and related attributes among sensory inputs can be accessed, and the perceptual decision can be made. A recent finding using MEG supports the account of dynamic and multiple competitive mechanisms (Kuo, Nobre, Scerif, & Astle, 2016). In their study, when participants searched for a target within an array, they first observed phase–phase coupling within the alpha band, between frontoparietal cortices and the visual areas. Importantly, this coupling corresponded to the spatial location of the target items, consistent with some early gating process. This alpha-band effect preceded the N2pc, as in the current study. Moreover, we showed that the amount of alpha phase adjustment was positively correlated with N2pc amplitude—further suggesting that these two mechanisms are functionally intertwined with each other. When T-N similarity is high, the target can be accessed and selected effectively if the similar nontargets can be suppressed beforehand or in parallel. Alongside these findings, the current results provide temporal markers for gating and spatiotopic access to the target representations during visual search.

In conclusion, we have isolated two electrophysiological effects that are sensitive to competition during visual search. We provided evidence showing that efficient search requires effective gating, which is reflected by alpha lateralization in phase adjustment. Along with that, target representations can be accessed and selected for making search decisions. Both processes are influenced by the competitive interaction between targets and nontargets.

Acknowledgments

This work was supported by a grant from the Ministry of Science and Technology, Taiwan (MOST 104-2628-H-002-002-MY3). The authors thank Duncan Astle for his comments and suggestions on an early version of the manuscript.

Reprint requests should be sent to Bo-Cheng Kuo, Department of Psychology, National Taiwan University, No. 1, Sec. 4, Roosevelt Road, 10617, Taipei, Taiwan, or via e-mail: bckuo@ntu.edu.tw.

REFERENCES

Aubin, S., & Jolicoeur, P. (2016). Early and late selection modulate competition for representation: Evidence from the N2pc in a multiple frame procedure. *Psychophysiology*, *53*, 611–622.

Bacigalupo, F., & Luck, S. J. (2019). Lateralized suppression of alpha-band EEG activity as a mechanism of target processing. *Journal of Neuroscience*, *39*, 900–917.

Beck, D. M., & Kastner, S. (2009). Top–down and bottom–up mechanisms in biasing competition in the human brain. *Vision Research*, *49*, 1154–1165.

Bonnefond, M., & Jensen, O. (2012). Alpha oscillations serve to protect working memory maintenance against anticipated distracters. *Current Biology*, *22*, 1969–1974.

Brignani, D., Lepsien, J., & Nobre, A. C. (2010). Purely endogenous capture of attention by task-defining features proceeds independently from spatial attention. *Neuroimage*, *51*, 859–866.

Bundesen, C. (1990). A theory of visual attention. *Psychological Review*, *97*, 523–547.

Busch, N. A., Dubois, J., & VanRullen, R. (2009). The phase of ongoing EEG oscillations predicts visual perception. *Journal of Neuroscience*, *29*, 7869–7876.

Buschman, T. J., & Kastner, S. (2015). From behavior to neural dynamics: An integrated theory of attention. *Neuron*, *88*, 127–144.

Chelazzi, L. (1999). Serial attention mechanisms in visual search: A critical look at the evidence. *Psychological Research*, *62*, 195–219.

Desimone, R., & Duncan, J. (1995). Neural mechanisms of selective visual attention. *Annual Review of Neuroscience*, *18*, 193–222.

Drisdelle, B. L., & Jolicoeur, P. (2018). Early and late selection processes have separable influences on the neural substrates of attention. *International Journal of Psychophysiology*, *127*, 52–61.

Dugué, L., Marque, P., & VanRullen, R. (2011). The phase of ongoing oscillations mediates the causal relation between brain excitation and visual perception. *Journal of Neuroscience*, *31*, 11889–11893.

Duncan, J., & Humphreys, G. W. (1989). Visual search and stimulus similarity. *Psychological Review*, *96*, 433–458.

Eimer, M. (1996). The N2pc component as an indicator of attentional selectivity. *Electroencephalography and Clinical Neurophysiology*, *99*, 225–234.

Eimer, M. (2014). The neural basis of attentional control in visual search. *Trends in Cognitive Sciences*, *18*, 526–535.

Eimer, M., & Grubert, A. (2014). Spatial attention can be allocated rapidly and in parallel to new visual objects. *Current Biology*, *24*, 193–198.

Feldmann-Wüstefeld, T., & Schubö, A. (2015). Target discrimination delays attentional benefit for grouped contexts: An ERP study. *Brain Research*, *1629*, 196–209.
Feldmann-Wüstefeld, T., Uengoer, M., & Schubö, A. (2015). You see what you have learned. Evidence for an interrelation of associative learning and visual selective attention. *Psychophysiology*, *52*, 1483–1497.
Feldmann-Wüstefeld, T., & Vogel, E. K. (2019). Neural evidence for the contribution of active suppression during working memory filtering. *Cerebral Cortex*, *29*, 529–543.
Feldmann-Wüstefeld, T., Wykowska, A., & Schubö, A. (2013). Context heterogeneity has a sustained impact on attention deployment: Behavioral and electrophysiological evidence. *Psychophysiology*, *50*, 722–733.
Foster, J. J., Sutterer, D. W., Serences, J. T., Vogel, E. K., & Awh, E. (2017). Alpha-band oscillations enable spatially and temporally resolved tracking of covert spatial attention. *Psychological Science*, *28*, 929–941.
Gaspelin, N., & Luck, S. J. (2018a). Combined electrophysiological and behavioral evidence for the suppression of salient distractors. *Journal of Cognitive Neuroscience*, *30*, 1265–1280.
Gaspelin, N., & Luck, S. J. (2018b). The role of inhibition in avoiding distraction by salient stimuli. *Trends in Cognitive Sciences*, *22*, 79–92.
Grubert, A., & Eimer, M. (2015). Rapid parallel attentional target selection in single-color and multiple-color visual search. *Journal of Experimental Psychology: Human Perception and Performance*, *41*, 86–101.
Haegens, S., Nácher, V., Luna, R., Romo, R., & Jensen, O. (2011). α-oscillations in the monkey sensorimotor network influence discrimination performance by rhythmical inhibition of neuronal spiking. *Proceedings of the National Academy of Sciences, U.S.A.*, *108*, 19377–19382.
Händel, B. F., Haarmeier, T., & Jensen, O. (2011). Alpha oscillations correlate with the successful inhibition of unattended stimuli. *Journal of Cognitive Neuroscience*, *23*, 2494–2502.
Hickey, C., Di Lollo, V., & McDonald, J. J. (2009). Electrophysiological indices of target and distractor processing in visual search. *Journal of Cognitive Neuroscience*, *21*, 760–775.
Hilimire, M. R., Mounts, J. R. W., Parks, N. A., & Corballis, P. M. (2009). Competitive interaction degrades target selection: An ERP study. *Psychophysiology*, *46*, 1080–1089.
Hopf, J.-M., Luck, S. J., Girelli, M., Hagner, T., Mangun, G. R., Scheich, H., et al. (2000). Neural sources of focused attention in visual search. *Cerebral Cortex*, *10*, 1233–1241.
Itti, L., & Koch, C. (2001). Computational modelling of visual attention. *Nature Reviews Neuroscience*, *2*, 194–203.
Jennings, J. R., & Wood, C. C. (1976). The epsilon-adjustment procedure for repeated-measures analyses of variance. *Psychophysiology*, *13*, 277–278.
Jensen, O., Bonnefond, M., & VanRullen, R. (2012). An oscillatory mechanism for prioritizing salient unattended stimuli. *Trends in Cognitive Sciences*, *16*, 200–206.
Jensen, O., & Mazaheri, A. (2010). Shaping functional architecture by oscillatory alpha activity: Gating by inhibition. *Frontiers in Human Neuroscience*, *4*, 186.
Kastner, S., & Ungerleider, L. G. (2000). Mechanisms of visual attention in the human cortex. *Annual Review of Neuroscience*, *23*, 315–341.
Kastner, S., & Ungerleider, L. G. (2001). The neural basis of biased competition in human visual cortex. *Neuropsychologia*, *39*, 1263–1276.
Kelly, S. P., Lalor, E. C., Reilly, R. B., & Foxe, J. J. (2006). Increases in alpha oscillatory power reflect an active retinotopic mechanism for distracter suppression during sustained visuospatial attention. *Journal of Neurophysiology*, *95*, 3844–3851.
Kiss, M., Van Velzen, J., & Eimer, M. (2008). The N2pc component and its links to attention shifts and spatially selective visual processing. *Psychophysiology*, *45*, 240–249.
Klimesch, W. (2012). Alpha-band oscillations, attention, and controlled access to stored information. *Trends in Cognitive Sciences*, *16*, 606–617.
Klimesch, W., Sauseng, P., & Hanslmayr, S. (2007). EEG alpha oscillations: The inhibition–timing hypothesis. *Brain Research Reviews*, *53*, 63–88.
Kuo, B.-C., Li, C.-H., Lin, S.-H., Hu, S.-H., & Yeh, Y.-Y. (2017). Top–down modulation of alpha power and pattern similarity for threatening representations in visual short-term memory. *Neuropsychologia*, *106*, 21–30.
Kuo, B.-C., Nobre, A. C., Scerif, G., & Astle, D. E. (2016). Top–down activation of spatiotopic sensory codes in perceptual and working memory search. *Journal of Cognitive Neuroscience*, *28*, 996–1009.
Kuo, B.-C., Rao, A., Lepsien, J., & Nobre, A. C. (2009). Searching for targets within the spatial layout of visual short-term memory. *Journal of Neuroscience*, *29*, 8032–8038.
Lavie, N., & Cox, S. (1997). On the efficiency of visual selective attention: Efficient visual search leads to inefficient distractor rejection. *Psychological Science*, *8*, 395–398.
Luck, S. J., Chelazzi, L., Hillyard, S. A., & Desimone, R. (1997). Neural mechanisms of spatial selective attention in areas V1, V2, and V4 of macaque visual cortex. *Journal of Neurophysiology*, *77*, 24–42.
Luck, S. J., & Hillyard, S. A. (1994). Spatial filtering during visual search: Evidence from human electrophysiology. *Journal of Experimental Psychology: Human Perception and Performance*, *20*, 1000–1014.
Maris, E., & Oostenveld, R. (2007). Nonparametric statistical testing of EEG- and MEG-data. *Journal of Neuroscience Methods*, *164*, 177–190.
Mathewson, K. E., Gratton, G., Fabiani, M., Beck, D. M., & Ro, T. (2009). To see or not to see: Prestimulus α phase predicts visual awareness. *Journal of Neuroscience*, *29*, 2725–2732.
Mazza, V., Turatto, M., & Caramazza, A. (2009). An electrophysiological assessment of distractor suppression in visual search tasks. *Psychophysiology*, *46*, 771–775.
Miller, J., Patterson, T., & Ulrich, R. (1998). Jackknife-based method for measuring LRP onset latency differences. *Psychophysiology*, *35*, 99–115.
Moran, J., & Desimone, R. (1985). Selective attention gates visual processing in the extrastriate cortex. *Science*, *229*, 782–784.
Mueller, S. T., & Weidemann, C. T. (2012). Alphabetic letter identification: Effects of perceivability, similarity, and bias. *Acta Psychologica*, *139*, 19–37.
Munneke, J., Fait, E., & Mazza, V. (2013). Attentional processing of multiple targets and distractors. *Psychophysiology*, *50*, 1104–1108.
Myers, N. E., Stokes, M. G., Walther, L., & Nobre, A. C. (2014). Oscillatory brain state predicts variability in working memory. *Journal of Neuroscience*, *34*, 7735–7743.
Nako, R., Smith, T. J., & Eimer, M. (2015). Activation of new attentional templates for real-world objects in visual search. *Journal of Cognitive Neuroscience*, *27*, 902–912.
Oldfield, R. C. (1971). The assessment and analysis of handedness: The Edinburgh inventory. *Neuropsychologia*, *9*, 97–113.
Olivers, C. N. L., Peters, J., Houtkamp, R., & Roelfsema, P. R. (2011). Different states in visual working memory: When it guides attention and when it does not. *Trends in Cognitive Sciences*, *15*, 327–334.

Oostenveld, R., Fries, P., Maris, E., & Schoffelen, J.-M. (2011). FieldTrip: Open source software for advanced analysis of MEG, EEG, and invasive electrophysiological data. *Computational Intelligence and Neuroscience*, *2011*, 156869.

Payne, L., Guillory, S., & Sekuler, R. (2013). Attention-modulated alpha-band oscillations protect against intrusion of irrelevant information. *Journal of Cognitive Neuroscience*, *25*, 1463–1476.

Payne, L., & Sekuler, R. (2014). The importance of ignoring: Alpha oscillations protect selectivity. *Current Directions in Psychological Science*, *23*, 171–177.

Reynolds, J. H., & Chelazzi, L. (2004). Attentional modulation of visual processing. *Annual Review of Neuroscience*, *27*, 611–647.

Reynolds, J. H., Chelazzi, L., & Desimone, R. (1999). Competitive mechanisms subserve attention in macaque areas V2 and V4. *Journal of Neuroscience*, *19*, 1736–1753.

Rihs, T. A., Michel, C. M., & Thut, G. (2009). A bias for posterior α-band power suppression versus enhancement during shifting versus maintenance of spatial attention. *Neuroimage*, *44*, 190–199.

Romei, V., Gross, J., & Thut, G. (2012). Sounds reset rhythms of visual cortex and corresponding human visual perception. *Current Biology*, *22*, 807–813.

Samaha, J., Sprague, T. C., & Postle, B. R. (2016). Decoding and reconstructing the focus of spatial attention from the topography of alpha-band oscillations. *Journal of Cognitive Neuroscience*, *28*, 1090–1097.

Sauseng, P., Klimesch, W., Heise, K. F., Gruber, W. R., Holz, E., Karim, A. A., et al. (2009). Brain oscillatory substrates of visual short-term memory capacity. *Current Biology*, *19*, 1846–1852.

Sawaki, R., Geng, J. J., & Luck, S. J. (2012). A common neural mechanism for preventing and terminating the allocation of attention. *Journal of Neuroscience*, *32*, 10725–10736.

Scalf, P. E., & Beck, D. M. (2010). Competition in visual cortex impedes attention to multiple items. *Journal of Neuroscience*, *30*, 161–169.

Tallon-Baudry, C., Bertrand, O., Delpuech, C., & Pernier, J. (1996). Stimulus specificity of phase-locked and non-phase-locked 40 Hz visual responses in human. *Journal of Neuroscience*, *16*, 4240–4249.

Thut, G., Nietzel, A., Brandt, S. A., & Pascual-Leone, A. (2006). α-band electroencephalographic activity over occipital cortex indexes visuospatial attention bias and predicts visual target detection. *Journal of Neuroscience*, *26*, 9494–9502.

Töllner, T., Gramann, K., Müller, H. J., Kiss, M., & Eimer, M. (2008). Electrophysiological markers of visual dimension changes and response changes. *Journal of Experimental Psychology: Human Perception and Performance*, *34*, 531–542.

Townsend, J. T. (1971). Theoretical analysis of an alphabetic confusion matrix. *Perception & Psychophysics*, *9*, 40–50.

Treisman, A. M., & Gelade, G. (1980). A feature-integration theory of attention. *Cognitive Psychology*, *12*, 97–136.

Treisman, A. M., & Gormican, S. (1988). Feature analysis in early vision: Evidence from search asymmetries. *Psychological Review*, *95*, 15–48.

van den Berg, B., Appelbaum, L. G., Clark, K., Lorist, M. M., & Woldorff, M. G. (2016). Visual search performance is predicted by both prestimulus and poststimulus electrical brain activity. *Scientific Reports*, *6*, 37718.

van Ede, F., Chekroud, S. R., Stokes, M. G., & Nobre, A. C. (2019). Concurrent visual and motor selection during visual working memory guided action. *Nature Neuroscience*, *22*, 477–483.

Wolfe, J. M. (1994). Guided Search 2.0 A revised model of visual search. *Psychonomic Bulletin & Review*, *1*, 202–238.

Woodman, G. F., Arita, J. T., & Luck, S. J. (2009). A cuing study of the N2pc component: An index of attentional deployment to objects rather than spatial locations. *Brain Research*, *1297*, 101–111.

Worden, M. S., Foxe, J. J., Wang, N., & Simpson, G. V. (2000). Anticipatory biasing of visuospatial attention indexed by retinotopically specific α-band electroencephalography increases over occipital cortex. *Journal of Neuroscience*, *20*, RC63.

Zelinsky, G. J., & Bisley, J. W. (2015). The what, where, and why of priority maps and their interactions with visual working memory. *Annals of the New York Academy of Sciences*, *1339*, 154–164.

Zumer, J. M., Scheeringa, R., Schoffelen, J.-M., Norris, D. G., & Jensen, O. (2014). Occipital alpha activity during stimulus processing gates the information flow to object-selective cortex. *PLoS Biology*, *12*, e1001965.